

Defect equilibrium in $\text{PrBaCo}_2\text{O}_{5+\delta}$ at elevated temperatures

A.Yu. Suntsov^{a,*}, I.A. Leonidov^{a,b}, M.V. Patrakeev^a, V.L. Kozhevnikov^a

^a Institute of Solid State Chemistry, Pervomaiskaya str.91, Ekaterinburg 620990, Russia

^b Ural Federal University, Mira str.19, Ekaterinburg, 620002 Russia

ARTICLE INFO

Article history:

Received 13 May 2013

Received in revised form

19 July 2013

Accepted 29 July 2013

Available online 9 August 2013

Keywords:

Praseodymium-barium cobaltites

Oxygen nonstoichiometry

$p\text{O}_2$ – T – δ diagram

Defect equilibrium

ABSTRACT

A defect equilibrium model for $\text{PrBaCo}_2\text{O}_{5+\delta}$ is suggested based on oxygen non-stoichiometry data. The model includes reactions of oxygen exchange and charge disproportionation of Co^{3+} cations. The respective equilibrium constants, enthalpies and entropies for the reactions entering the model are obtained from the fitting of the experimental data for oxygen non-stoichiometry. The enthalpies of oxidation $\text{Co}^{2+} \rightarrow \text{Co}^{3+}$ and $\text{Co}^{3+} \rightarrow \text{Co}^{4+}$ are found to be equal to $115 \pm 9 \text{ kJ mol}^{-1}$ and $45 \pm 4 \text{ kJ mol}^{-1}$, respectively. The obtained equilibrium constants were used in order to calculate variations in concentration of cobalt species with non-stoichiometry, temperature and oxygen pressure.

© 2013 Elsevier Inc. All rights reserved.

1. Introduction

Substitution of lanthanide (*Ln*) for alkali-earth metals in perovskite-like cobaltites LnCoO_3 results in formation of extended solid solutions and deviations (δ) of oxygen content from stoichiometric composition. In difference with Ca or Sr substituted cobaltites where doping cations randomly replace lanthanide cations within the entire solubility range, the larger barium cations tend to ordering so that composition $\text{Ln}_{0.5}\text{Ba}_{0.5}\text{CoO}_{3-\delta}$ is characterized by alternation of *Ln* and Ba cations along *c*-axis [1–4]. Consequently, the elementary unit parameters *a*, *b* and *c* for $\text{Ln}_{0.5}\text{Ba}_{0.5}\text{CoO}_{3-\delta}$ approximately relate with the elementary unit parameter a_p for the parent perovskite-like cobaltite as a_p , $2a_p$ and $2a_p$, respectively, while the obtained oxides are called “double perovskite” cobaltites and their chemical formula is usually represented as $\text{LnBaCo}_2\text{O}_{5+\delta}$.

The interesting feature of the double perovskite cobaltites $\text{LnBaCo}_2\text{O}_{5+\delta}$ is a large homogeneous range δ of oxygen content that may vary within $0 \leq \delta \leq 1$ depending on temperature and oxygen partial pressure in the ambient atmosphere [2,5,6]. Notice that the partial filling of the sites available for oxygen exchange is a prerequisite for large mobility of oxygen ions in the crystalline lattice. At the same time, the presence of cobalt cations that can easily change their oxidation state is favorable for electron conductivity [7–9]. Therefore, the double perovskite cobaltites have attracted considerable interest in recent years from the researchers in the field of catalysis, adsorption and cathode materials [10–19]. It is known that the respective functional properties are tightly related with the nature of electron and ion

defects in non-stoichiometric oxides, in general, and in the double-perovskite cobaltites, in particular. The data on charge states, ion association and other information pertaining to defect structure are usually obtained from the analysis of pressure and temperature dependences of oxygen stoichiometry in the range of elevated temperatures, where thermodynamic equilibrium can be attained in a reasonably short time [20]. However, the literature concerning oxygen content in the double-perovskite cobaltites at high-temperatures is quite scarce. In turn, the lack of the respective data makes it difficult to understand electric properties, and thus facilitate the application of double-perovskite cobaltites.

It is widely recognized that electric properties in cobaltites are strongly influenced by charge disproportionation of Co^{3+} and appearance of Co^{2+} and Co^{4+} cations [7,8]. We have shown earlier [21] with the using of $\text{PrBaCo}_2\text{O}_{5+\delta}$ as an example that all three charged cobalt species can simultaneously coexist in the double perovskite cobaltites at large variations of oxygen content. However, the previous defect model [21] was essentially based on calculations of the concentration of cobalt species from oxygen stoichiometry only while the influence of temperature on their equilibrium was introduced indirectly via temperature dependence of thermopower. In this work the effect of temperature on defect equilibria is taken into account directly through the using of respective equilibrium constants. It is found that a good correspondence of the defect model and thermodynamic data can be achieved when the influence of the crystalline environment upon charge state of cobalt cations is taken into account.

2. Experimental

The samples of $\text{PrBaCo}_2\text{O}_{5+\delta}$ were obtained by solid state synthesis from high purity oxides Pr_6O_{11} and Co_3O_4 , and barium

* Corresponding author. Fax: +7 343 3744495.

E-mail address: suntsov@ihim.uran.ru (A.Yu. Suntsov).

carbonate BaCO_3 . The respective mixture was thoroughly ground with a mortar and pestle, pelletized and calcined in air at 900–1150 °C. The procedure was repeated several times with the gradual increase of the firing temperature. After heating during 24 h at the final stage, the specimens were slowly cooled down to room temperature.

The phase purity control and determination of crystal lattice parameters at room temperature were carried out by powder X-ray diffraction with the using of a Stadi-P (Stoe) diffractometer equipped with $\text{CuK}\alpha$ -radiation. The air synthesized cobaltite $\text{PrBaCo}_2\text{O}_{5+\delta}$ was confirmed to be a single phase (Fig. 1) having an orthorhombic structure (space group $Pmmm$) with the unit cell parameters $a=3.8981(1)$, $b=7.8069(2)$ and $c=7.6345(2)$ Å characteristic of a double perovskite [1–4]. A part of the obtained $\text{PrBaCo}_2\text{O}_{5+\delta}$ was crashed into a thin powder and used for determination of absolute amount of oxygen in the as-prepared material. The powder sample was placed in a Setaram TG-92 thermoanalyzer and heated to 1000 °C in the atmosphere containing 90% He and 10% H_2 . As a result of the reducing heat treatment, the specimen had been reduced to metallic cobalt, barium oxide and praseodymium sesquioxide, and the total weight loss was sufficient to calculate oxygen content in the starting, i.e. as-prepared, specimen. The oxygen non-stoichiometry parameter $\delta=0.77$ in as-synthesized samples was found to be in agreement with earlier results [22]. Then, the change of the oxygen content in the as-prepared specimen at heating in air was determined with the help of the thermoanalyzer. The heating rate was 5 °C/min and the heating mode included long term isothermal steps at 650, 700, ..., 950 °C to ensure perfect equilibration of the weight change, i.e. oxygen content in the specimen, with the temperature increase.

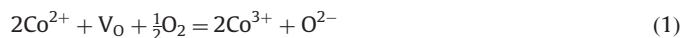
The oxygen content variations in $\text{PrBaCo}_2\text{O}_{5+\delta}$ at different values of temperature T and partial pressure of oxygen $p\text{O}_2$ were obtained using a coulometric titration technique in the isothermal regime. The equilibrium criterion of the titration isotherms was selected change in $\log(p\text{O}_2/\text{atm})$ less than $2 \times 10^{-4}/\text{min}$. The measurements were carried out within oxygen partial pressure range 3×10^{-4} –1 atm and at temperatures between 650 and 950 °C. The temperature interval between the titration isotherms was 50 °C. The uncertainty in measured δ values did not exceed $\Delta\delta = \pm 0.001$. The value of the oxygen content at 650 °C, which was obtained at TG heating of the as-prepared sample in air, was utilized as a reference point for the coulometric titration isotherm at $p\text{O}_2=0.21$ atm and 650 °C. The excellent match of the coulometric and TG data at other temperature values employed in the coulometric measurements demonstrates reliability of the

employed coulometric titration technique. Additional experimental details are described elsewhere [23,24].

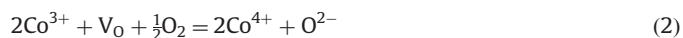
3. Results and discussion

3.1. Defect equilibrium model

The experimentally obtained dependencies of the total oxygen content ($5+\delta$) in $\text{PrBaCo}_2\text{O}_{5+\delta}$ at different temperatures and oxygen pressure values are shown in Fig. 2. The parameter ($5+\delta$) varies from 5.2 to 5.55 within the studied limits of T and $p\text{O}_2$. When heated in He the cobaltite acquires tetragonal structure (S.G. $P4/mmm$) [25] with $\delta=0.48$ at 503 °C. Similar structural transition near 500 °C was observed also in other rare-earth cobaltites $\text{LnBaCo}_2\text{O}_{5+\delta}$, where $\text{Ln}=\text{Nd}, \text{Sm}, \text{Gd}$ [26,27]. Therefore, the isothermal dependencies of oxygen content ($5+\delta$) vs. $p\text{O}_2$ in Fig. 2 ($p\text{O}_2$ – T – δ diagram) pertain to tetragonal phase modification of $\text{PrBaCo}_2\text{O}_{5+\delta}$. The smooth shape of the isotherms gives additional evidence to the absence of phase transitions in $\text{PrBaCo}_2\text{O}_{5+\delta}$ within the studied range of oxygen pressure and temperature values; the stability of tetragonal structure at elevated temperatures is due to randomization of oxygen ions O^{2-} and vacancies V_O over O3 positions [25–27]. Simple consideration of charge balance suggests coexistence of Co^{2+} and Co^{3+} cations mostly in $\text{PrBaCo}_2\text{O}_{5+\delta}$ at $\delta < 0.5$. Therefore, the primary reaction of oxygen intake and oxidation can be represented as



Only when $\delta > 0.5$ deeper oxidation of cobalt and appearance of Co^{4+} cations may occur



The transition from extremely reduced to extremely oxidized state of cobalt cations is given by the sum of reactions (1) and (2)



Moreover, heating can facilitate charge redistribution over cobalt cations



Electron- and hole-type carriers, i.e. Co^{2+} and Co^{4+} cations, in $\text{LnBaCo}_2\text{O}_{5+\delta}$ were reported earlier [7,8]. Accordingly, the coexistence of charged cobalt species in the cobaltite can be reflected in the formula $\text{PrBaCo}_n^{2+}\text{Co}_z^{3+}\text{Co}_p^{4+}\text{O}_{5+\delta}$ where symbols n , z and p denote concentration per formula unit of respective cobalt cations. The vacancy concentration in $\text{PrBaCo}_2\text{O}_{5+\delta}$ can be obtained as

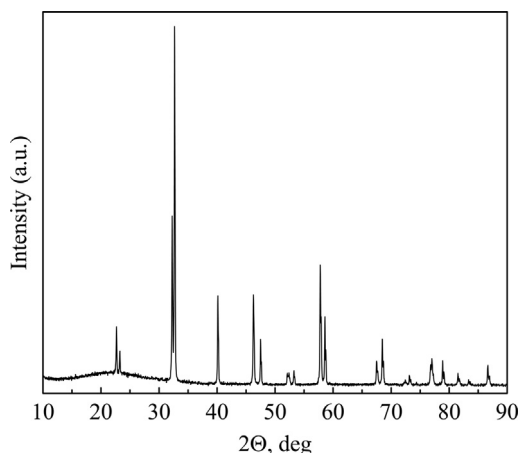


Fig. 1. The experimental X-ray powder diffraction pattern of air-synthesized $\text{PrBaCo}_2\text{O}_{5+\delta}$, $\delta=0.77$.

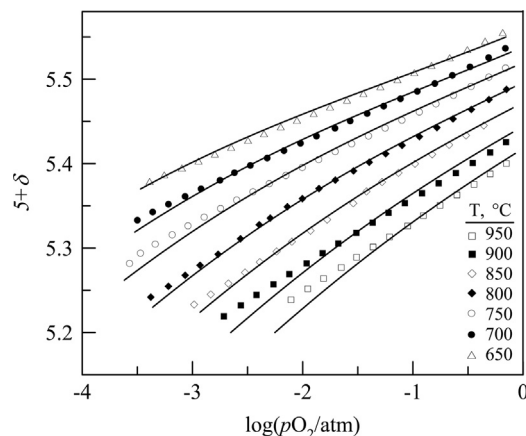


Fig. 2. Isothermal plots for oxygen content vs. oxygen partial pressure over $\text{PrBaCo}_2\text{O}_{5+\delta}$. Solid lines show calculation results according to Eq. (11).

$[V_O]=1-\delta$. Then the equilibrium constants for reactions (3) and (4) can be presented as

$$K_{Ox} = \frac{p(5+\delta)}{n(1-\delta)p_{O_2}^{1/2}} \quad (5)$$

$$K_D = \frac{np}{z^2} \quad (6)$$

The site conservation and charge neutrality requirements can be respectively expressed as

$$n + z + p = 2 \quad (7)$$

$$p = n + 2\delta - 1 \quad (8)$$

Then, δ dependent concentrations of cobalt species follow from (6)–(8) as

$$p = \frac{4K_D + 8K_D\delta - 2\delta + 1 - \sqrt{D}}{8K_D - 2} \quad (9)$$

$$n = p - 2\delta + 1, \quad z = 2 - n - p \quad (10)$$

where symbol D is stand for

$$D = 12K_D + 4\delta^2 - 16K_D\delta^2 - 4\delta + 16K_D\delta + 1$$

The equilibrium pressure of oxygen over $\text{PrBaCo}_2\text{O}_{5+\delta}$ can be expressed from (5) as

$$p_{O_2}^{1/2} = \frac{1}{K_{Ox}} \frac{(5+\delta)p}{(1-\delta)n} \quad (11)$$

with p and n taken from (9) and (10), respectively. Eq. (11) gives a convenient expression for simulation of the experimental p_{O_2} – T – δ diagram in Fig. 2 with the using of two independent fitting parameters K_{Ox} and K_D . The respective results of the fitting are shown in Fig. 2 with solid lines. It is seen that the suggested equilibrium defect model gives a very good description of the experimental isotherms at 650–750 °C while small divergence of the theoretical and experimental data can be observed at higher temperatures and $p_{O_2} < 0.01$ atm. The equilibrium constants K_{Ox} and K_D obtained from the fitting are shown in Arrhenius coordinates in Fig. 3. The linear shape of the plots enables calculation of the standard enthalpy ΔH_j° and entropy ΔS_j° values for reactions (3) and (4) with the help of the known relation

$$-RT \ln K_j = \Delta G_j^\circ = \Delta H_j^\circ - T \Delta S_j^\circ \quad (12)$$

The correspondingly calculated results are shown in Table 1. Moreover, reactions (1) and (2) can be obtained by combining reactions (3) and (4). Therefore, the thermodynamic functions for the oxidation reactions of Co^{2+} and Co^{3+} cations can be respectively calculated (Table 1). Taking in view the oxidation enthalpy smaller in reaction (1) than in (2), we come to conclusion that the

Table 1
Thermodynamic parameters for equilibrium reactions in $\text{PrBaCo}_2\text{O}_{5+\delta}$.

Reaction	ΔH° (kJ mol ^{−1})	ΔS° (J mol ^{−1} K ^{−1})
$2\text{Co}^{3+} = \text{Co}^{2+} + \text{Co}^{4+}$	35 ± 4	-12 ± 2
$\text{Co}^{2+} + V_O + \frac{1}{2}\text{O}_2 = \text{Co}^{4+} + \text{O}^{2-}$	-80 ± 5	-55 ± 3
$2\text{Co}^{2+} + V_O + \frac{1}{2}\text{O}_2 = 2\text{Co}^{3+} + \text{O}^{2-}$	-115 ± 9	-43 ± 2
$2\text{Co}^{3+} + V_O + \frac{1}{2}\text{O}_2 = 2\text{Co}^{4+} + \text{O}^{2-}$	-45 ± 4	-67 ± 5

oxygen intake and oxidation reaction of the cobaltite $\text{PrBaCo}_2\text{O}_{5+\delta}$ at $\delta \approx 0$ takes place, first of all, at the expense of Co^{2+} cations and their oxidation to Co^{3+} cations. Only in a more oxidized state where concentration of Co^{3+} cations in $\text{PrBaCo}_2\text{O}_{5+\delta}$ is large enough oxidation of Co^{3+} to Co^{4+} cations may occur. It should be noted that the oxidation enthalpy -45 ± 4 kJ mol^{−1} in reaction (2) almost exactly equals a half of the partial enthalpy of oxygen $h_{O_2}^\circ$ obtained recently in the similar cobaltite $\text{GdBaCo}_2\text{O}_{5+\delta}$ [19]. At the same time authors [28] arrived to the conclusion that the $\text{Co}^{4+} \rightarrow \text{Co}^{3+}$ reduction process in $\text{GdBaCo}_2\text{O}_{5+\delta}$ is accompanied with the enthalpy change of 240.6 kJ mol^{−1}. This value seems to be unusually large in comparison with the data in [19] and our results for $\text{PrBaCo}_2\text{O}_{5+\delta}$. It also seems to be overestimated in comparison with the redox enthalpy in the cubic perovskite-like cobaltite $\text{La}_{0.5}\text{Sr}_{0.5}\text{CoO}_{3-\delta}$ where it achieves only about 100 kJ mol^{−1} [20] and with the similar value in $\text{La}_{0.6}\text{Sr}_{0.4}\text{CoO}_{3-\delta}$ [29]. Our estimation in Table 1 appears to be in a more favorable comparison with the data for $\text{La}_{1-x}\text{Sr}_x\text{CoO}_{3-\delta}$ because smaller absolute value for oxidation enthalpy of $\text{PrBaCo}_2\text{O}_{5+\delta}$ in reaction (2) can naturally be explained as due to crystalline structure less dense in the double perovskite – than in the simple perovskite-like cobaltites. For instance, the room temperature volume of the reduced elementary unit in $\text{PrBaCo}_2\text{O}_{5.5}$ equals 58.6 \AA^3 [25] while the elementary unit volume in $\text{La}_{0.6}\text{Sr}_{0.4}\text{CoO}_{3-\delta}$ is 56.4 \AA^3 [29]. The difference reflects shorter and stronger bonds Co–O and, therefore, oxidation enthalpy larger in $\text{La}_{0.6}\text{Sr}_{0.4}\text{CoO}_{3-\delta}$ than in $\text{PrBaCo}_2\text{O}_{5+\delta}$.

The charge disproportionation enthalpy 35 kJ mol^{−1} in our defect model for $\text{PrBaCo}_2\text{O}_{5+\delta}$ is close to the respective value 37 kJ mol^{−1} in $\text{LaCoO}_{3-\delta}$ [30]. It must be noted also that the obtained ΔH_D° is approximately equal, as expected, to the energy gap between t_{2g} and e_g levels in the rare-earth double perovskite cobaltites [31]. The using of the negative enthalpy $\Delta H_D^\circ = -24.4$ kJ mol^{−1} obtained from the defect model in [28] would lead to a strong decrease in the amount of Co^{3+} cations with temperature so that their concentration would become negligently small at near room temperatures. Such a conclusion occurs in a strong controversy with the available literature data [1–4].

3.2. Changes in concentration of cobalt cations

The equilibrium constants and Eqs.(7), (9), and (10) enable one to calculate variations in concentration n , z and p of cobalt species in $\text{PrBaCo}_n^{2+}\text{Co}_z^{3+}\text{Co}_p^{4+}\text{O}_{5+\delta}$ with δ , T and p_{O_2} (Fig. 4). It is seen that changes in the charge state of Co^{3+} cations are most pronounced at $(5+\delta)=5.5$. The temperature increase is accompanied with the appreciable increase in concentration of Co^{2+} and Co^{4+} cations, and in simultaneous decline in concentration of Co^{3+} cations. The isothermal changes in concentration of Co^{2+} cations vary as $n \approx 1 - 2\delta$ at $\delta \rightarrow 0$ whereas the concentration of holes, i.e. Co^{4+} cations, depends on the non-stoichiometry parameter as $p \approx 2\delta - 1$ at $\delta \rightarrow 1$. The concentration of Co^{3+} cations approaches unity in both extremes $\delta \rightarrow 0$ and $\delta \rightarrow 1$ (Fig. 4). The opposite trend can be observed at temperature decrease. Calculations with the help of (9) and (10) show that the concentration of Co^{2+} and Co^{4+} cations in $\text{PrBaCo}_2\text{O}_{5.5}$ achieves only about 0.05 per formula unit at temperatures near 500 °C, i.e., at the low-temperature stability

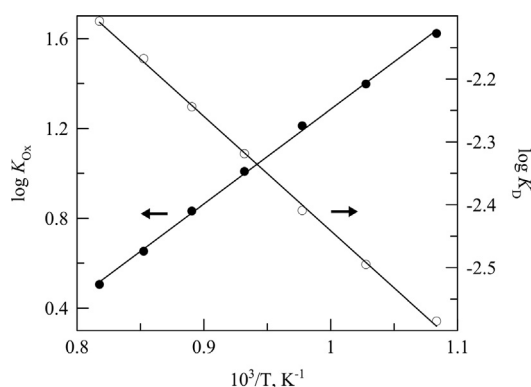


Fig. 3. Logarithmic dependencies of equilibrium constants from inverse temperature.

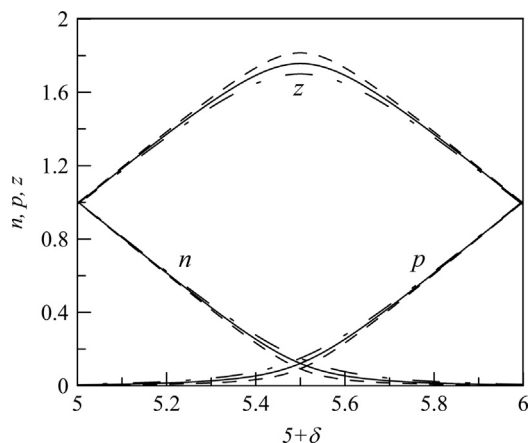


Fig. 4. Variations in concentration of cobalt species with oxygen content in PrBaCo₂O_{5+δ} at 650 °C (dashed line), 800 °C (solid line), and 950 °C (dash-dotted line).

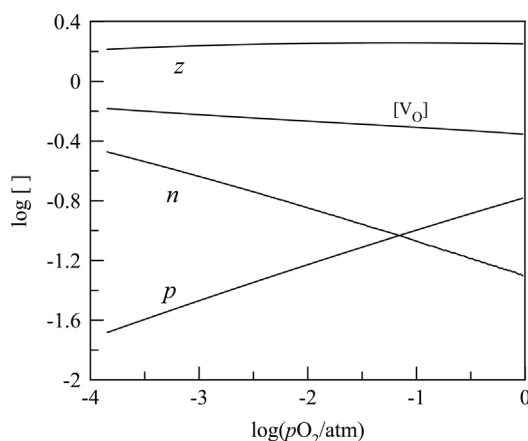


Fig. 5. Oxygen pressure dependent variations in concentration of cobalt species and oxygen vacancies in PrBaCo₂O_{5+δ} at 650 °C.

border of the tetragonal structure. Further decrease of the temperature results in even stronger suppression of reaction (4), and concentration of Co²⁺ and Co⁴⁺ cations becomes so small that they can hardly be detected by, e.g., spectral methods. However, our conclusion is clearly supported by large thermopower at near room temperatures [8], which is clearly indicative of a very small concentration of charge carriers.

The pressure dependent changes in concentration of cobalt cations and oxygen vacancies at 650 °C are shown in logarithmic coordinates in Fig. 5. It is seen clearly that electron–hole equilibrium at this temperature is attained at $pO_2 \approx 0.1$ atm, i.e. at pressure and temperature values that provide the fulfillment of the condition $\delta = 0.5$. At the same time, the sign of thermopower in PrBaCo₂O_{5+δ} remains always positive thus demonstrating p-type dominant charge carriers in the studied intervals of T and pO_2 even when $\delta < 0.5$ [21]. The hole-type conductivity at elevated temperatures was observed also in other double perovskite cobaltites LnBaCo₂O_{5+δ} [26,32,33]. Thus, even in conditions where n-type carriers are more numerous than p-type ones they provide smaller contribution to conductivity in PrBaCo₂O_{5+δ}. Therefore, mobility of electrons must be considerably smaller than of holes. This difference may originate from larger bond length Co²⁺–O²⁻ (2.01 Å) compared to Co⁴⁺–O²⁻ (1.93 Å) [34]. Moreover, it is easier for holes to jump over filled Co³⁺ ($t_{2g}^4 e_g^2$) and empty Co⁴⁺ ($t_{2g}^5 e_g^0$) states than for electrons over filled Co³⁺ ($t_{2g}^4 e_g^2$) and Co²⁺ ($t_{2g}^6 e_g^0$) states.

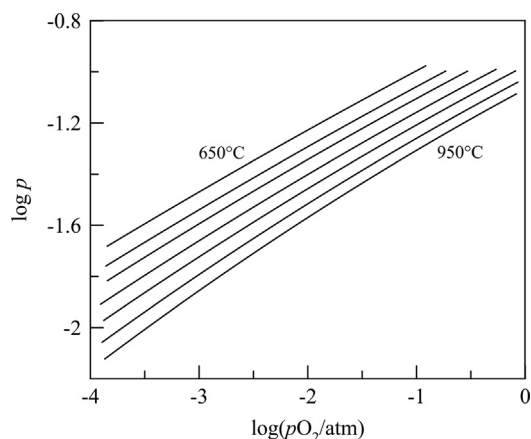


Fig. 6. Calculated changes in concentration of Co⁴⁺ cations with oxygen pressure at different temperatures.

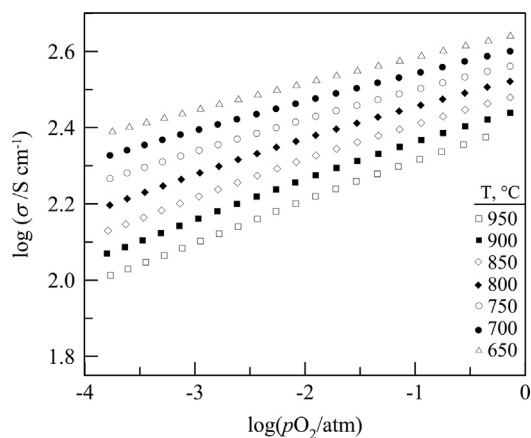


Fig. 7. The plots log σ vs. log pO₂ at different temperatures.

The isothermal changes in the concentration of holes with oxygen pressure are shown in Fig. 6. The temperature increase at $pO_2 = \text{const}$ is accompanied with the decrease in the concentration of holes and, respectively, conductivity (Fig. 7). This behavior reflects rather strong changes in concentration of holes with oxygen non-stoichiometry (Fig. 4).

Considering reaction (4) we can suppose that it is favored when Co³⁺ cations occupy neighboring sites in the crystalline lattice. It occurs most often at largest concentration of Co³⁺ cations in PrBaCo₂O_{5+δ}, i.e. at δ near 0.5. The deviation from this composition results in the decrease of Co³⁺ concentration and, consequently, probability to find neighboring Co³⁺ cations. Hence, the intensity of charge disproportionation (4) is expected to decrease at $\delta \rightarrow 1$ and $\delta \rightarrow 0$ compared to $\delta = 0.5$. This effect is completely disregarded in our treatment of the defect equilibrium in PrBaCo₂O_{5+δ}. Therefore, the errors in calculated concentrations of cobalt species are expected to increase at $\delta \rightarrow 0$. In turn, the increased errors may help to explain the observed deviations of the calculated (5+δ) values compared to the measured ones in the low pressure limit in Fig. 2.

4. Conclusions

The analysis of oxygen non-stoichiometry changes with temperature and partial pressure of oxygen is used in order to show that oxygen exchange and charge disproportionation reactions take place in defect equilibrium in PrBaCo₂O_{5+δ}. The respective

equilibrium constants, enthalpies and entropies for the reactions entering the model are derived from the fitting of the experimental data for oxygen non-stoichiometry. The variations in concentration of cobalt species with temperature, oxygen pressure and oxygen content in $\text{PrBaCo}_2\text{O}_{5+\delta}$ are calculated with the help of the obtained equilibrium constants. It is argued that charge disproportionation of Co^{3+} cations is most developed at $\delta=0.5$.

Acknowledgments

Authors gratefully acknowledge partial support of this work by the Russian Foundation for Basic Research (Grant no. 12-03-31570) and the Ministry of Education and Science of the Russian Federation (Grant no. 8649).

References

- [1] I.O. Troyanchuk, N.V. Kasper, D.D. Khalyavin, H. Szymczak, R. Szymczak, M. Baran, *Phys. Rev. Lett.* 80 (1998) 3380–3383.
- [2] A. Maignan, C. Martin, D. Pelloquin, N. Nguyen, B. Raveau, *J. Solid State Chem.* 142 (1999) 247–260.
- [3] T. Vogt, P.M. Woodward, P. Karen, B.A. Hunter, P. Henning, A.R. Moodenbaugh, *Phys. Rev. Lett.* 84 (2000) 2969–2972.
- [4] D. Akahoshi, Y. Ueda, *J. Solid State Chem.* 156 (2001) 355–363.
- [5] N.V. Kasper, I.O. Troyanchuk, D.D. Khalyavin, N. Hamad, L. Haupt, P. Fröbel, K. Bärner, E. Gmelin, Q. Huang, J.W. Lynn, *Phys. Stat. Sol. (b)* 215 (1999) 697–701.
- [6] V. Pralong, V. Caignaert, S. Hebert, A. Maignan, B. Raveau, *Solid State Ionics* 177 (2006) 1879–1881.
- [7] A. Maignan, V. Caignaert, B. Raveau, D. Khomskii, G. Sawatzky, *Phys. Rev. Lett.* 93 (2004) 026401.
- [8] A.A. Taskin, A.N. Lavrov, Y. Ando, *Phys. Rev. Lett.* 95 (2005) 176603.
- [9] M.A. Señas-Rodríguez, J.B. Goodenough, *J. Solid State Chem.* 116 (1995) 224–231.
- [10] J. Pena-Martinez, A. Tarancon, D. Marrero-Lopez, J.C. Ruiz-Morales, P. Nunez, *Fuel Cells* 8 (2008) 351–359.
- [11] G. Kim, S. Wang, A.J. Jacobson, L. Reimus, P. Brodersen, C.A. Mims, *Mater. Chem.* 17 (2007) 2500–2505.
- [12] A. Tarancon, D. Marrero-Lopez, J. Pena-Martinez, J.C. Ruiz-Morales, P. Nunez, *Solid State Ionics* 179 (2008) 611–618.
- [13] D.J. Chen, R. Ran, K. Zhang, J. Wang, Z.P. Shao, *J. Power Sources* 188 (2009) 96–105.
- [14] K. Zhang, L. Ge, R. Ran, Z.P. Shao, S.M. Liu, *Acta Mater.* 56 (2008) 4876–4889.
- [15] M. Burriel, J. Pena-Martinez, R.J. Chater, S. Fearn, A.V. Berenov, S.J. Skinner, J.A. Kilner, *Chem. Mater.* 24 (2012) 613–621.
- [16] A. Tarancon, A. Chroneos, D. Parfit, J.A. Kilner, *Solid Oxide Fuel Cells* 35 (2011) 1151–1154.
- [17] Y.F. He, X.F. Zhu, Q.M. Li, W.S. Yang, *AIChE J.* 55 (2009) 3125–3133.
- [18] Q.H. Yin, J. Kniep, Y.S. Lin, *Chem. Eng. Sci.* 63 (2008) 5870–5875.
- [19] L. Moggi, F. Prado, C. Jimenez, A. Caneiro, *Solid State Ionics* 240 (2013) 19–28.
- [20] M. Kuhn, S. Hashimoto, K. Sato, K. Yashiro, J. Mizusaki, *J. Solid State Chem.* 197 (2013) 38–45.
- [21] A.Y. Suntsov, I.A. Leonidov, M.V. Patrakeev, V.L. Kozhevnikov, *J. Solid State Chem.* 184 (2011) 1951–1955.
- [22] C. Frontera, A. Caneiro, A.E. Carrillo, J. Oro-Sole, J.L. García-Muñoz, *Chem. Mater.* 17 (2005) 5439–5445.
- [23] M.V. Patrakeev, E.B. Mitberg, A.A. Lakhtin, I.A. Leonidov, V.L. Kozhevnikov, V.V. Kharton, M. Avdeev, F.M.B. Marques, *J. Solid State Chem.* 167 (2002) 203–213.
- [24] M.V. Patrakeev, I.A. Leonidov, V.L. Kozhevnikov, *J. Solid State Electrochem.* 15 (2011) 931–954.
- [25] S. Streule, A. Podlesnyak, D. Sheptyakov, E. Pomjakushina, M. Stingaciu, K. Conder, M. Medarde, M.V. Patrakeev, I.A. Leonidov, V.L. Kozhevnikov, *J. Mesot. Phys. Rev. B* 73 (2006) 094203.
- [26] A. Tarancon, D. Marrero-Lopez, J. Peña-Martinez, J.C. Ruiz-Morales, P. Nunez, *Solid State Ionics* 179 (2008) 611–618.
- [27] J.-H. Kim, L. Moggi, F. Prado, A. Caneiro, J.A. Alonso, A. Manthiram, *J. Electrochem. Soc.* 156 (2009) B1376–B1382.
- [28] D.S. Tsvetkov, V.V. Sereda, A.Y. Zuev, *Solid State Ionics* 180 (2010) 1620–1625.
- [29] M. Søgaard, P.V. Hendriksen, M. Mogensen, *J. Solid State Chem.* 180 (2007) 1487–1503.
- [30] S.R. Sehlin, H.U. Anderson, D.M. Sparlin, *Phys. Rev. B* 52 (1995) 11681–11689.
- [31] H. Wu, *Phys. Rev. B* 64 (2001) 092413.
- [32] T.V. Aksenova, L.Y. Gavrilova, A.A. Yaremchenko, V.A. Cherepanov, V.V. Kharton, *Mater. Res. Bull.* 45 (2010) 1288–1292.
- [33] D.A. Medvedev, T.A. Zhuravleva, A.A. Murashkina, V.S. Sergeeva, B.D. Antonov, *Russ. J. Phys. Chem. A* 84 (2010) 1623–1627.
- [34] R.D. Shannon, *Acta Crystallogr. A* 32 (1976) 751–767.